ADVANCED BEAM DYNAMICS EXPERIMENTS WITH THE SPARC HIGH BRIGHTNESS PHOTOINJECTOR

M. Ferrario, D. Alesini, F. Anelli, M. Bellaveglia, M. Boscolo, L. Cacciotti, M. Castellano, E. Chiadroni, L. Cultrera, G. Di Pirro, L. Ficcadenti, D. Filippetto, S. Fioravanti, A. Gallo, G. Gatti, E. Pace, R. Sorchetti, A. Mostacci, C. Vaccarezza, INFN-LNF, Frascati, RM, Italy
L. Giannessi, A. Petralia, C. Ronsivalle, ENEA C.R. Frascati, RM, Italy
A. Bacci, V. Petrillo, A.R. Rossi, L. Serafini, INFN-Mi, Milano, Italy
O. Limaj, M. Moreno, M. Serluca, INFN-Roma I, Roma, Italy
A. Cianchi, B. Marchetti, INFN-Roma II, Roma, Italy
C. Vicario, PSI, Villigen Switzerland
J. Rosenzweig, UCLA, Los Angeles, CA, USA
H. Tomizawa, SPring-8/JASRI, Japan

Abstract

The recent successful operation of the SPARC injector in the Velocity Bunching (VB) mode has opened new perspectives to conduct advanced beam dynamics experiments with ultra-short electron pulses able to extend the THz spectrum and to drive the FEL in the SASE Single Spike mode. In addition a new technique called Laser Comb, able to generate a train of short pulses with high repetition rate, has been recently tested in the VB configuration. In this paper we report the experimental results obtained so far.

INTRODUCTION

One of the main goals of the SPARC photoinjector is the generation of short electron bunches with the velocity bunching technique [1,2]. The longitudinal phase space rotation in the velocity bunching process is based on a correlated time-velocity chirp in the electron bunch, so that electrons on the tail of the bunch are faster than electrons in the bunch head. This rotation occurs inside the longitudinal potential of a traveling radio frequency (RF) wave (longitudinal focusing), which accelerates the beam inside a long multi-cell RF structure and simultaneously applies an off-crest energy chirp to the injected beam. To keep the space charge effects under control when the bunch is compressed, the first two S-band traveling wave accelerating structures, downstream of the 1.6-cell S-band RF gun, are embedded in long solenoids. An RF deflecting cavity placed at the exit of the third accelerating structure allows bunch length and slice emittance measurements [3]. When the downstream dipole is switched on a direct measurement of the longitudinal trace space is also possible.

With this machine configuration, other advanced beam manipulation schemes can be investigated, such as the so-called "laser comb" concept [4,5]. In this injector operating mode, the photocathode is illuminated by a comb-like laser pulse in order to produce a train of sub-picosecond high-charge density pulses within the same RF gun accelerating bucket. Downstream of the gun exit, each pulse develops a space charge induce linear energy chirp, typical of the blow out regime [6], which can be exploited to compress the initial charge profile either by means of an RF accelerating structure, operating in the velocity bunching mode, or by a magnetic compressor with a negative R_{56}. Electron pulse trains with some hundreds pC charge, a sub-picosecond length, and a repetition rate of some terahertz can be used to drive pump and probe free-electron laser (FEL) experiments [7], coherent excitation of plasma waves in plasma accelerators [8], generation of narrow-band terahertz radiation [9,10], and other beam dynamics studies [11]. In addition the laser comb modulation being driven by a longitudinal plasma wave oscillation, can be considered like a giant micro-bunch instability or a beam-echo effect and can give deep insights to study also this interesting beam physics phenomena.

In this paper, we describe the laser system upgrade and the experimental results achieved so far at SPARC.

SPARC LASER SYSTEM

The SPARC laser system [12] is based on a Ti:Sa oscillator that generates 130-*fs* pulses with a repetition rate of 79+1/3 MHz, synchronous with the accelerating RF field at 2856 MHz. For the laser comb experiment, the required pulse shape is characterized by two or more short pulses spaced by a few picoseconds. The technique used for this purpose relies on a birefringent crystal, where the input pulse is decomposed in two orthogonally polarized pulses with a time separation proportional to the crystal length. If more birefringent glasses are inserted in the laser beam path, it is possible to produce a more dense comb structure. For the measurement reported in this paper, the UV stretcher has been bypassed, and the short UV pulses have been sent to the birefringent crystal. The crystal is α-cut beta barium borate (BBO), which is a UV transparent optical material characterized by a strong birefringence. The α-BBO crystals are oriented with fast and slow axes at 45° with respect to the incident horizontal polarization, so that a single pulse is equally split into two pulses, with the orthogonal polarizations traveling at different group velocities in each crystal. Since the crystal has its optical axis parallel to the front surfaces, there is no spatial walk-off between the ordinary and extraordinary beams, and the output pulses are naturally aligned. The induced separation between the pulses is: $\Delta\tau = (n_o - n_e)L_1/c$, where L_1 is the BBO length, n_o and n_e are the ordinary and extraordinary indexes of refraction at the wavelength of 266 nm, and c is the speed of light. To change the relative intensity of the pulses, a remotely controlled half-waveplate is inserted before the BBO.

LONGITUDINAL BEAM DYNAMICS

The main purpose of the first experiment (September 2009) with SPARC in the laser comb configuration was to study the longitudinal dynamics and the compression ratio as a function of the injection phase in the velocity bunching [13]. The laser system has been set up to produce two pulses with a low charge per pulse in order to reduce the space charge effects and to avoid external focusing (long solenoid off).

We have been operating with two Gaussian longitudinal laser profiles (shown in Fig. 1) that are 0.65-ps rms long separated by 8.2 ps with 300 μm of transverse spot size. The total extracted charge was 70 pC (~35 pC/pulse) with a 15% charge unbalance between the two pulses. The peak field in the RF gun was 100 MV/m, and the extraction phase was 32°. When the beam was accelerated on crest by an accelerating field of 21 MV/m in the first two sections and 11 MV/m in the last section, the final energy was 164 MeV with a 300-keV energy separation between the two pulses. The rms pulse lengths measured at the linac exit were 0.77 ps and 0.86 ps respectively, and the pulse separation was 6.5 ps. In the compression regime, the beam energy was observed to progressively decrease to 110 MeV, with the total energy spread increasing up to 1 %. Under these experimental conditions, the resolution of the bunch length measurements was ~ 100 fs.

Table 1. Measured pulse length [ps]

Phase	Trailing Pulse	Leading Pulse	Pulse distance
0°	0.73 ±0.01	0.83 ±0.04	6.50 ±0.02
-80°	0.13 ± 0.01	0.40 ± 0.01	2.79 ±0.24
-89°	0.19 ± 0.07	0.22 ± 0.02	Overlapped
-93°	0.11 ± 0.11	0.17 ±0.02	1.24 ±0.24

Table 1 reports the measured rms pulse length and the pulse distance versus the injection phase in the first traveling wave structure for the four different conditions we have investigated: on crest (0°), moderate compression (-80°), maximum compression (-89°), and over-compression (-93°). The measurement uncertainty, statistically computed over 10 shots, is also reported. In Fig. 1, the corresponding instantaneous current profiles, as measured at the linac exit, are shown. The low charge per pulse (~ 35 pC) made it difficult to reconstruct the absolute value of the current.

A significant beam compression (distance between the two pulses) occurs only after a phase shift of -80° degrees. In the next 8° injection phase shift, the strong compression regime occurs, thus progressively reducing the pulse distance up to a full overlapping of the original separated pulses.

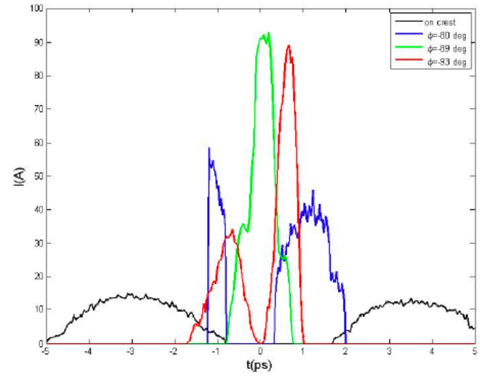

Fig. 1. Two pulses, instantaneous current profiles at the linac exit, as reconstructed by the measuremets: on crest (0°, black line); moderate compression (-80°, blue); maximum compression (-89°, green); and over-compression (-93°, red).

The over-compression regime occurs for the injection phases that exceed -89°, the two pulses are again separated, and the time order is inverted. The single pulse compression curves show a delay with respect to the beam compression curve [13]. The trailing bunch experiences maximum compression at -91°, and the leading bunch 6° later.

TRANSVERSE BEAM DYNAMICS

During the second experiment performed at SPARC (May 2010) in the laser comb configuration, we focused our investigation on the transverse beam dynamics, in order to demonstrate the possibility to keep under control with the external focusing system (the long solenoid placed around the VB structure) the emittance growth of such a particular two pulses configuration.

We have been operating with two Gaussian pulses, with σ_t = 0.3 ps separated by 4 ps with 400 μm of transverse spot size. The total extracted charge was increased up 180 pC (~90 pC/pulse).

PARMELA simulations show that with an injection phase in the VB close to -93° and a proper tuning of the external focusing elements it is possible to balance the output current and emittance of both pulses, as shown in Fig. 2. It is interesting to note that such a configurations corresponds also to the minimum of the total projected emittance, as seen in the transverse phase spaces shown in the boxes of Fig. 2. This is certainly a simplification of the optimization process during the experiments since the measurement of the total projected emittance is quite a fast procedure. The slice emittance measurement is the only way to get direct information about the transverse beam quality of each pulse. In the SPARC configuration it can be done only for one plane (orizontal) and it takes a longer time.

Following the PARMELA indications, and after optimizing the phases of the accelerating sections and the solenoids field strength, we observed on the screen downstream the RF deflector-dipole system the longitudinal trace space, see Fig. 3, clearly showing two electron bunches separated by ~0.9 ps with σ_{t1} = 0.24 ps and σ_{t2} =0.29 ps respectively. The final average energy was 111 MeV with an energy difference between the two pulses of ~ 2 MeV. The corresponding energy profile is shown if Fig. 4. The rms energy spread within two pulses was 0.3 % and 0.7 % respectively.

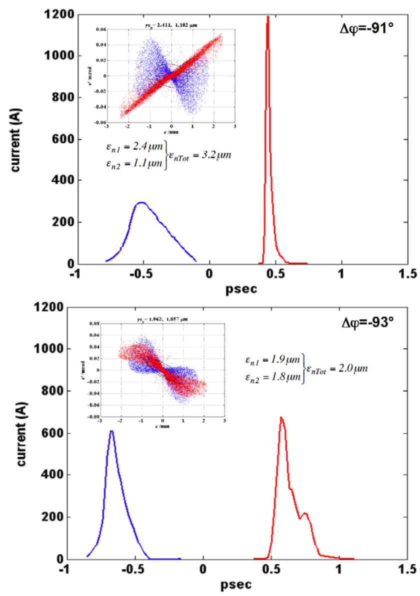

Fig. 2. Current profiles of the two pulses at the linac exit (PARMELA simulations) for different injection phases in the VB: -91^{o} upper plot, -93^{o} lower plot. The corresponding transverse phase spaces are shown in the small boxes.

We performed also a slice emittance measurements of the two pulses as reported in Fig. 5, showing an orizontal emittance of ~3 μm and ~4 μm respectively, corresponding to a total measured projected emittance under this condition of ~ 4 μm in both planes. The corresponding normalized charge profile shows a current unbalance of about 40 %, indicating that there was still some room for optimization. Notice that the higher current pulse has the lower emittance due to a likely better matching with in the linac.

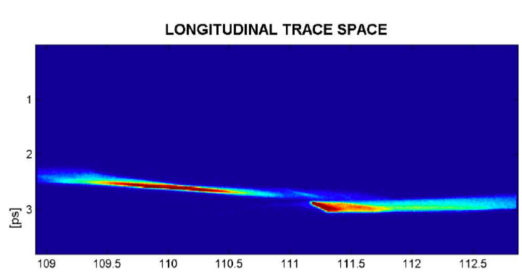

Fig. 3. Longitudinal trace space of the comb beam at the linac exit, VB injection phase -93^{o}

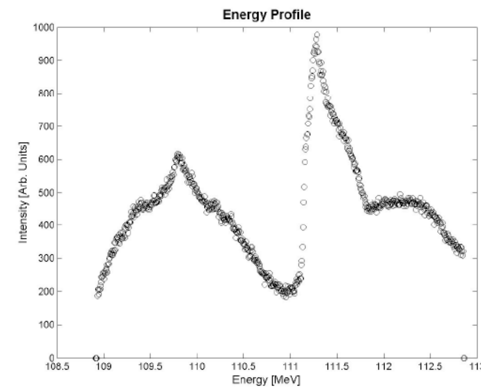

Fig. 4. energy profile of the comb beam at the linac exit, VB injection phase -93^{o}

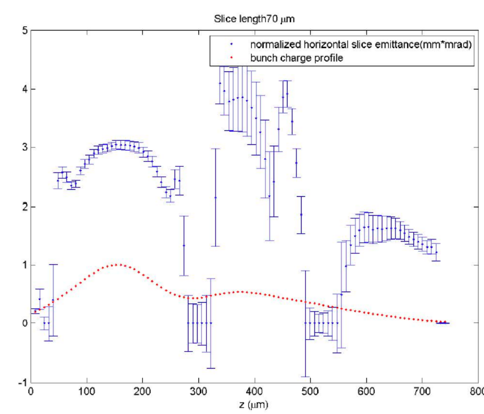

Fig. 5. Slice emittance measurement of the comb beam reconstructed for a fixed slice length of 70 μm. VB injection phase -93^{o}. The corresponding normalized charge profile is also shown (red curve)

REFERENCES

[1] L. Serafini, M. Ferrario, AIP Conference Proceedings, 581, 87 (2001).
[2] M. Ferrario et al., Phys. Rev. Lett. **104**, 054801 (2010).
[3] D. Alesini, et al., Proc. of DIPAC 2009, Basel, Switzerland (2009).
[4] P.O.Shea, et al., Proc. of 2001 IEEE PAC, Chicago, IL, USA (2001) p.704.
[5] M. Boscolo, et al., Int. J. Mod. Phys. B 21, p. 415 February 2007.
[6] P. Musumeci et al., Phys. Rev. ST Accel. Beams 12, 070704 (2009)
[7] M. Boscolo, et al. Nucl. Instr. & Meth. In Phys. Res. A, **593**, August 2008, pp. 106-110.
[8] P. Muggli et al., Phys. Rev. Lett. 101, 054801 (2008).
[9] J. G. Neumann et al., Journal of Appl. Physics **105**, 053304 (2009).
[10] E. Chiadroni et al., Proc. of IPAC 2010, Kyoto, Japan, (2010).
[11] P. Piot, et al., PRST-AB 9, 053501 (2006).
[12] C. Vicario, et al., Proc. PAC 2007, Albuquerque, NM, USA, (2007).
[13] M. Ferrario et al., Nucl. Inst. and Meth. A, in press: doi:10.1016/j.nima.2010.02.018